

Photoproduction of Jets and Heavy Flavors in Polarized ep - Collisions at HERA[†]

M. Stratmann^a, W. Vogelsang^b

^a Universität Dortmund, Institut für Physik, D-44221 Dortmund, Germany

^b Rutherford Appleton Laboratory, Chilton, Didcot, Oxon OX11 0QX, England

Abstract: We study photoproduction of jets and heavy flavors in a polarized ep collider mode of HERA at $\sqrt{s} = 298$ GeV. We examine the sensitivity of the cross sections and their asymmetries to the proton's polarized gluon distribution and to the completely unknown parton distributions of longitudinally polarized photons.

1 Introduction

HERA has already been very successful in pinning down the proton's unpolarized gluon distribution $g(x, Q^2)$. Several processes have been studied which have contributions from $g(x, Q^2)$ already in the lowest order, such as (di)jet and heavy flavor production. Since events at HERA are concentrated in the region $Q^2 \rightarrow 0$, the processes have first and most accurately been studied in photoproduction [1-6]. As is well-known, in this case the (quasi-real) photon will not only interact in a direct ('point-like') way, but can also be resolved into its hadronic structure. HERA photoproduction experiments like [1-4] have not merely established evidence for the existence of such a resolved contribution, but have also been precise enough to improve our knowledge about the parton distributions, f^γ , of the photon.

Given the success of such unpolarized photoproduction experiments at HERA, it seems most promising [7] to closely examine the same processes for the situation with longitudinally polarized beams with regard to their sensitivity to the proton's polarized gluon distribution Δg , which is still one of the most interesting, but least known, quantities in 'spin-physics'. Recent next-to-leading (NLO) studies of polarized DIS [8, 9] show that the x -shape of Δg seems to be hardly constrained at all by the present DIS data [10], even though a tendency towards a sizeable positive *total* gluon polarization, $\int_0^1 \Delta g(x, Q^2 = 4 \text{ GeV}^2) dx \gtrsim 1$, was found [8, 11, 9]. Furthermore, polarized photoproduction experiments may in principle allow to not only determine the parton, in particular gluon, content of the polarized *proton*, but also that of the longitudinally polarized *photon* which is completely unknown so far. Since, e.g., a measurement of the photon's spin-dependent structure function g_1^γ in polarized e^+e^- collisions is not planned in the near future, HERA could play a unique role here, even if it should only succeed in establishing the very *existence* of a resolved contribution to polarized photon-proton reactions.

Our contribution is organized as follows: In section 2 we collect the necessary ingredients for our calculations. Section 3 is devoted to open-charm photoproduction. In section 4 we examine polarized photoproduction of (di)jets. Section 5 contains the conclusions.

[†]Contribution to the proceedings of the workshop on 'Future Physics at HERA', DESY, Hamburg, 1995/96.

2 Polarized Parton Distributions of the Proton and the Photon

Even though NLO analyses of polarized DIS which take into account all or most data sets [10] have been published recently [8, 11, 9], we have to stick to LO calculations throughout this work since the NLO corrections to polarized charm or jet production are not yet known. This implies use of LO parton distributions, which have also been provided in the studies [8, 9]. Both papers give various LO sets which mainly differ in the x -shape of the polarized gluon distribution. We will choose the LO 'valence' set of the 'radiative parton model analysis' [8], which corresponds to the best-fit result of that paper, along with two other sets of [8] which are based on either assuming $\Delta g(x, \mu^2) = g(x, \mu^2)$ or $\Delta g(x, \mu^2) = 0$ at the low input scale μ of [8], where $g(x, \mu^2)$ is the unpolarized LO GRV [12] input gluon distribution. These two sets will be called ' $\Delta g = g$ input' and ' $\Delta g = 0$ input' scenarios, respectively. The gluon of set C of [9] is qualitatively different since it has a substantial negative polarization at large x . We will therefore also use this set in our calculations. For illustration, we show in Fig. 1 the gluon distributions of the four different sets of parton distributions we will use, taking a typical scale $Q^2 = 10 \text{ GeV}^2$. Keeping in mind that all four LO sets provide very good descriptions of all present polarized DIS data [10], it becomes obvious that the data indeed do not seem to be able to significantly constrain the x -shape of $\Delta g(x, Q^2)$.

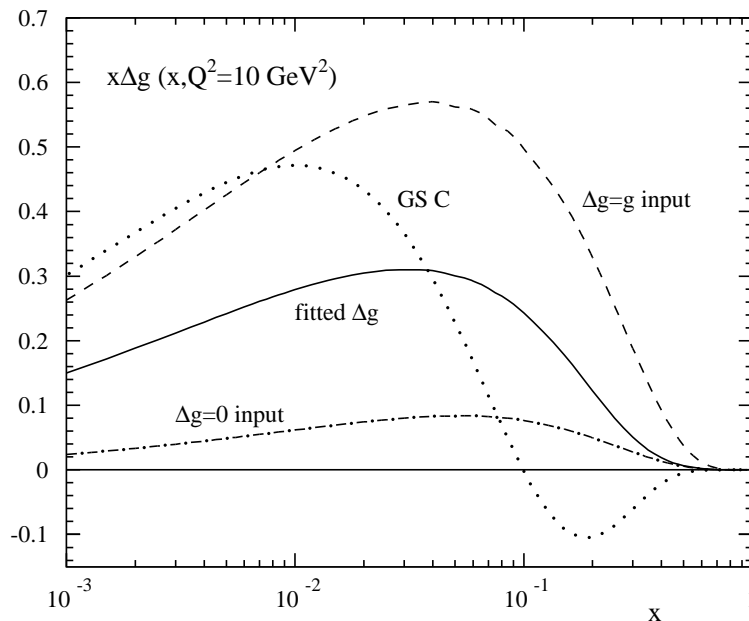


Figure 1: *Gluon distributions at $Q^2 = 10 \text{ GeV}^2$ of the four LO sets of polarized parton distributions used in this paper. The dotted line refers to set C of [9], whereas the other distributions are taken from [8] as described in the text.*

In the case of photoproduction the electron just serves as a source of quasi-real photons which are radiated according to the Weizsäcker-Williams spectrum [13]. The photons can then interact either directly or via their partonic structure ('resolved' contribution). In the case of longitudinally polarized electrons, the resulting photon will be longitudinally (more precisely, circularly) polarized and, in the resolved case, the *polarized* parton distributions of the photon, $\Delta f^\gamma(x, Q^2)$, enter the calculations. Thus one can define the effective polarized parton densities

at the scale M in the longitudinally polarized electron via¹

$$\Delta f^e(x_e, M^2) = \int_{x_e}^1 \frac{dy}{y} \Delta P_{\gamma/e}(y) \Delta f^\gamma(x_\gamma = \frac{x_e}{y}, M^2) \quad (1)$$

($f = q, g$) where $\Delta P_{\gamma/e}$ is the polarized Weizsäcker-Williams spectrum for which we will use

$$\Delta P_{\gamma/e}(y) = \frac{\alpha_{em}}{2\pi} \left[\frac{1 - (1 - y)^2}{y} \right] \ln \frac{Q_{max}^2(1 - y)}{m_e^2 y^2}, \quad (2)$$

with the electron mass m_e . For the time being, it seems most sensible to follow as closely as possible the analyses successfully performed in the unpolarized case, which implies to introduce the same kinematical cuts. As in [2, 4, 5, 14] we will use an upper cut² $Q_{max}^2 = 4 \text{ GeV}^2$, and the y -cuts $0.2 \leq y \leq 0.85$ (for charm and single-jet [2] production) and $0.2 \leq y \leq 0.8$ (for dijet production, [4]) will be imposed. We note that a larger value for the lower limit, y_{min} , of the allowed y -interval would enhance the yield of polarized photons relative to that of unpolarized ones since $\Delta P_{\gamma/e}(y)/P_{\gamma/e}(y)$, where $P_{\gamma/e}$ is the unpolarized Weizsäcker-Williams spectrum obtained by using $[(1 + (1 - y)^2)/y]$ instead of the square bracket in (2), is suppressed for small y . On the other hand, increasing y_{min} would be at the expense of reducing the individual polarized and unpolarized rates.

The polarized photon structure functions $\Delta f^\gamma(x_\gamma, M^2)$ in (1) are completely unmeasured so far, such that models for them have to be invoked. To obtain a realistic estimate for the theoretical uncertainties in the polarized photonic parton densities two very different scenarios were considered in [15, 16] assuming 'maximal' ($\Delta f^\gamma(x, \mu^2) = f^\gamma(x, \mu^2)$) or 'minimal' ($\Delta f^\gamma(x, \mu^2) = 0$) saturation of the fundamental positivity constraints $|\Delta f^\gamma(x, \mu^2)| \leq f^\gamma(x, \mu^2)$ at the input scale μ for the QCD evolution. Here μ and the unpolarized photon structure functions $f^\gamma(x, \mu^2)$ were adopted from the phenomenologically successful radiative parton model predictions in [17]. The results of these two extreme approaches are presented in Fig. 2 in terms of the photonic parton asymmetries $A_f^\gamma \equiv \Delta f^\gamma/f^\gamma$, evolved to $Q^2 = 30 \text{ GeV}^2$ in LO. An ideal aim of measurements in a polarized collider mode of HERA would of course be to determine the Δf^γ and to see which ansatz is more realistic. The sets presented in Fig. 2, which we will use in what follows, should in any case be sufficient to study the sensitivity of the various cross sections to the Δf^γ , but also to see in how far they influence a determination of Δg .

We finally note that in what follows a polarized cross section will always be defined as

$$\Delta\sigma \equiv \frac{1}{2} (\sigma(++)) - \sigma(+-)) , \quad (3)$$

the signs denoting the helicities of the scattering particles. The corresponding unpolarized cross section is given by taking the sum instead, and the cross section asymmetry is $A \equiv \Delta\sigma/\sigma$. Whenever calculating an asymmetry A , we will use the LO GRV parton distributions for the proton [12] and the photon [17] to calculate the unpolarized cross section. For consistency, we will employ the LO expression for the strong coupling α_s with [8, 9, 15, 16] $\Lambda_{QCD}^{(f=4)} = 200 \text{ MeV}$ for four active flavors.

¹We include here the additional definition $\Delta f^\gamma(x_\gamma, M^2) \equiv \delta(1 - x_\gamma)$ for the direct ('unresolved') case.

²In H1 analyses of HERA photoproduction data [1, 3, 6] the cut $Q_{max}^2 = 0.01 \text{ GeV}^2$ is used along with slightly different y -cuts as compared to the corresponding ZEUS measurements [2, 4, 5], which leads to smaller rates.

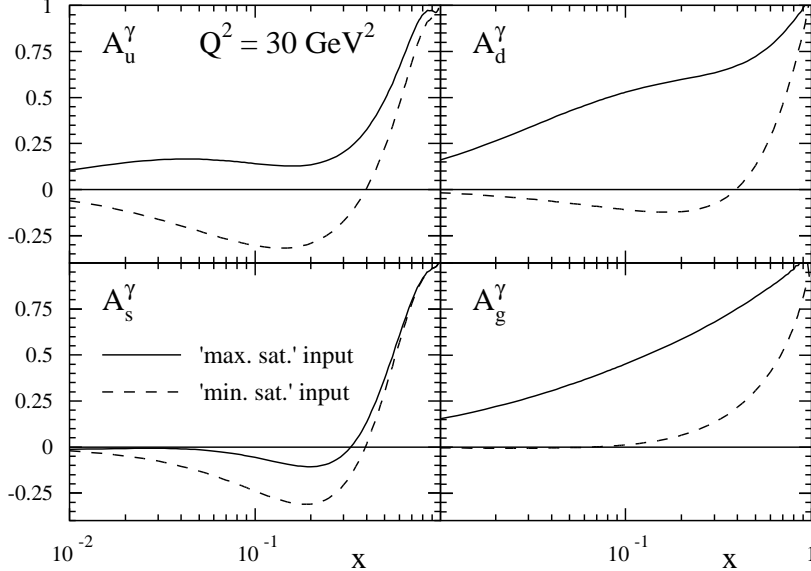


Figure 2: *Photonic LO parton asymmetries* $A_f^\gamma \equiv \Delta f^\gamma / f^\gamma$ at $Q^2 = 30 \text{ GeV}^2$ for the two scenarios considered in [15, 16] (see text). The unpolarized LO photonic parton distributions were taken from [17].

3 Charm Photoproduction at HERA

For illustration, we first briefly consider the total cross section. In the unpolarized case it has been possible to extract the total cross section for $\gamma p \rightarrow c\bar{c}$ from the fixed target [18] and HERA [5, 6] lepton-nucleon data, i.e., the open-charm cross section for a fixed photon energy without the smearing from the Weizsäcker-Williams spectrum. To LO, the corresponding polarized cross section is given by

$$\Delta\sigma^c(S_{\gamma p}) = \sum_{f^\gamma, f^p} \int_{4m_c^2/S_{\gamma p}}^1 dx_\gamma \int_{4m_c^2/x_\gamma S_{\gamma p}}^1 dx_p \Delta f^\gamma(x_\gamma, M^2) \Delta f^p(x_p, M^2) \Delta\hat{\sigma}^c(\hat{s}, M^2). \quad (4)$$

where M is some mass scale and $\hat{s} \equiv x_\gamma x_p S_{\gamma p}$. The Δf^p stand for the polarized parton distributions of the proton. In the direct case, the contributing subprocess is photon-gluon fusion (PGF), $\gamma g \rightarrow c\bar{c}$, whose spin-dependent total LO subprocess cross section $\Delta\hat{\sigma}^c(\hat{s})$ can be found in [19, 20]. In the resolved case, the processes $gg \rightarrow c\bar{c}$ and $q\bar{q} \rightarrow c\bar{c}$ contribute; their cross sections have been calculated in [21]. Needless to say that we can obtain the corresponding unpolarized LO charm cross section $\sigma^c(S_{\gamma p})$ by using LO unpolarized parton distributions and subprocess cross sections (as calculated in [22]) in (4).

Tab. 1 shows our results [7] for the polarized cross sections and the asymmetries $\Delta\sigma^c/\sigma^c$ for the four different sets of polarized parton distributions, where we have used the scale $M = 2m_c$ with the charm mass $m_c = 1.5 \text{ GeV}$. The resolved contribution to the cross section is rather small in the unpolarized case. For the polarized case, we have calculated it using the 'maximally' saturated set for the polarized photon structure functions, which should roughly provide the maximally possible background from resolved photons. The corresponding results are shown individually in Tab. 1. The resolved contribution turns out to be non-negligible only for large $\sqrt{S_{\gamma p}}$, where it can be as large as about 1/3 the direct contribution but with opposite sign. As becomes obvious from Tab. 1 (see also [23] and Fig. 4 of [7]), the asymmetry becomes very small towards the HERA region at larger $\sqrt{S_{\gamma p}} \sim 200 \text{ GeV}$. One reason for this is the oscillation of

the polarized subprocess cross section for the direct part, combined with cancellations between the direct and the resolved parts. More importantly, as seen from (4), the larger $S_{\gamma p}$ becomes, the smaller are the $x_{p,\gamma}$ - values probed, such that the rapid rise of the unpolarized parton distributions strongly suppresses the asymmetry. The smallness of the asymmetries and the possibly significant influence of the resolved contribution on them will make their measurement and a distinction between the different Δg elusive³. The measurement of the *total* charm cross section asymmetry in $\gamma p \rightarrow c\bar{c}$ seems rather more feasible at smaller energies, $\sqrt{S_{\gamma p}} \lesssim 20$ GeV, i.e., in the region accessible by the future COMPASS experiment [24] where also the unknown resolved contribution to the cross section is negligible.

$\sqrt{S_{\gamma p}}$ [GeV]	fitted Δg			$\Delta g = g$ input			$\Delta g = 0$ input			GS C		
	dir. [nb]	res. [nb]	A [%]	dir. [nb]	res. [nb]	A [%]	dir. [nb]	res. [nb]	A [%]	dir. [nb]	res. [nb]	A [%]
20	13.9	-0.29	2.6	23.2	0.33	4.5	3.26	-0.56	0.52	19.6	-0.70	3.6
50	2.07	1.30	0.18	1.15	2.94	0.21	-0.53	0.18	-0.019	17.4	0.61	0.94
200	-7.00	2.06	-0.06	-12.8	3.60	-0.11	-1.96	0.44	-0.018	-8.79	3.23	-0.067

Table 1: *Total cross sections and asymmetries A for charm photoproduction in polarized γp collisions.*

From our observations for HERA-energies it follows that it could be more promising to study distributions of the cross section in the transverse momentum or the rapidity of the charm quark in order to cut out the contributions from very small $x_{p,\gamma}$. We will now include the Weizsäcker-Williams spectrum since tagging of the electron, needed for the extraction of the cross section at fixed photon energy, will probably reduce the cross section too strongly. The polarized LO cross section for producing a charm quark with transverse momentum p_T and cms-rapidity η then reads

$$\frac{d^2\Delta\sigma^c}{dp_T d\eta} = 2p_T \sum_{f^e, f^p} \int_{\frac{\rho e^{-\eta}}{1-\rho e^\eta}}^1 dx_e x_e \Delta f^e(x_e, M^2) x_p \Delta f^p(x_p, M^2) \frac{1}{x_e - \rho e^{-\eta}} \frac{d\Delta\hat{\sigma}}{d\hat{t}}, \quad (5)$$

where $\rho \equiv m_T/\sqrt{S}$ with $m_T \equiv \sqrt{p_T^2 + m_c^2}$, and $x_p \equiv x_e \rho e^\eta / (x_e - \rho e^{-\eta})$. The cross section can be transformed to the more relevant HERA laboratory frame by a simple boost which implies $\eta \equiv \eta_{cms} = \eta_{LAB} - \frac{1}{2} \ln(E_p/E_e)$, where we have, as usual, counted positive rapidity in the proton forward direction. The spin-dependent differential LO subprocess cross sections $d\Delta\hat{\sigma}/d\hat{t}$ for the resolved processes $gg \rightarrow c\bar{c}$ and $q\bar{q} \rightarrow c\bar{c}$ with $m_c \neq 0$ can again be found in [21]. For the factorization/renormalization scale in (5) we choose $M = m_T/2$; we will comment on the scale dependence of the results at the end of this section.

Fig. 3 shows our results [7] obtained for the four different sets of polarized parton distributions for $E_p = 820$ GeV and $E_e = 27$ GeV. Fig. 3a displays the p_T -dependence of the cross section, where we have integrated over $-1 \leq \eta_{LAB} \leq 2$. The resolved contribution to the cross section has been included, calculated with the 'maximally' saturated set of polarized photon structure functions. It is shown individually for the 'fitted Δg '-set of polarized proton distributions by the lower solid line in Fig. 3a. Comparison of the two solid lines in Fig. 3a shows that

³As was shown in [23], the situation at HERA energies somewhat improves if cuts on the produced charm quark's transverse momentum and rapidity are imposed. However, the polarized resolved contribution to the asymmetry was neglected in [23].

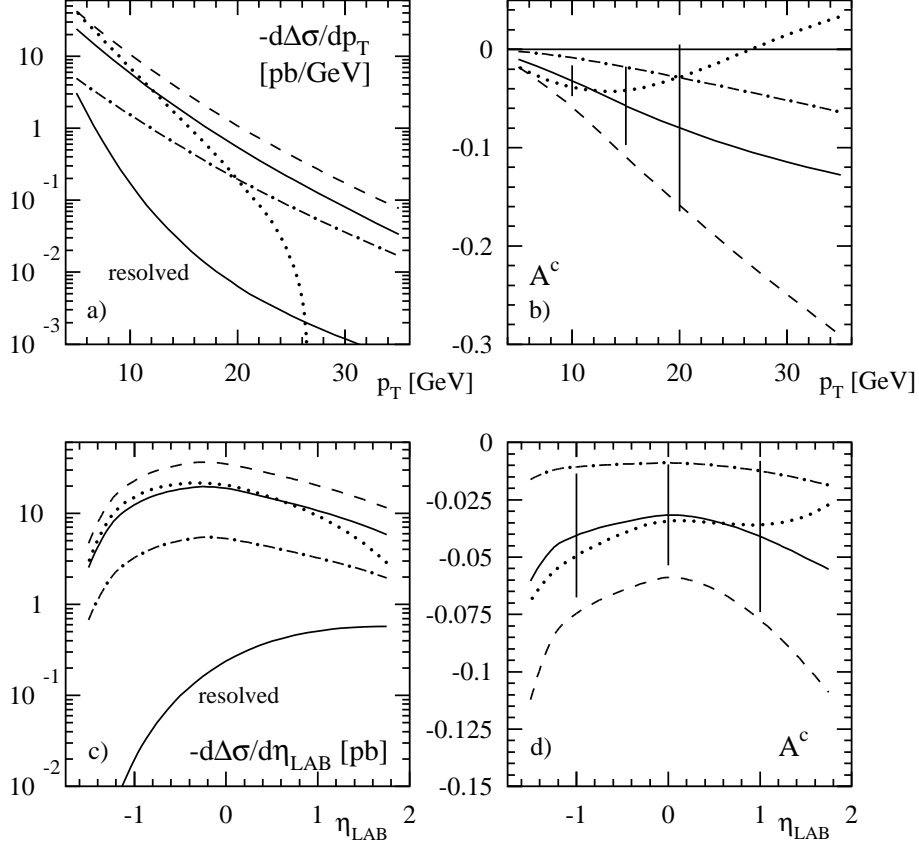


Figure 3: **a:** p_T -dependence of the (negative) polarized charm-photoproduction cross section in ep -collisions at HERA, calculated according to (5) (using $M = m_T/2$ and $m_c = 1.5$ GeV) and integrated over $-1 \leq \eta_{LAB} \leq 2$. The line drawings are as in Fig. 1. For comparison the resolved contribution to the cross section, calculated with the 'fitted Δg ' gluon distribution of [8] and the 'maximally' saturated set of polarized photonic parton distributions is shown by the lower solid line. **b:** Asymmetry corresponding to **a**. The expected statistical errors indicated by the bars have been calculated according to (6) and as explained in the text. **c,d:** Same as **a,b**, but for the η_{LAB} -dependence, integrated over $p_T > 8$ GeV.

the resolved contribution is negligibly small in this case unless p_T becomes very small. Fig. 3b shows the asymmetries corresponding to Fig. 3a. It becomes obvious that they are much larger than for the total cross section if one goes to p_T of about 10-20 GeV, which is in agreement with the corresponding findings of [23]. Furthermore, one sees that the asymmetries are strongly sensitive to the size *and* shape of the polarized gluon distribution used. Similar statements are true for the η_{LAB} -distributions shown in Figs. 3c,d, where p_T has been integrated over $p_T > 8$ GeV in order to increase the number of events. Even here the resolved contribution remains small, although it becomes more important towards large positive values of η_{LAB} . We have included in the asymmetry plots in Figs. 3b,d the expected statistical errors δA at HERA which can be estimated from

$$\delta A = \frac{1}{P_e P_p \sqrt{\mathcal{L} \sigma \epsilon}}, \quad (6)$$

where P_e , P_p are the beam polarizations, \mathcal{L} is the integrated luminosity and ϵ the charm detection efficiency, for which we assume $P_e * P_p = 0.5$, $\mathcal{L} = 100/\text{pb}$ and $\epsilon = 0.15$. The error bars in Fig. 3b,d have been obtained by integrating the unpolarized LO cross sections $d\sigma/dp_T$

or $d\sigma/d\eta_{LAB}$ over bins of $\Delta p_T = 5$ GeV or $\Delta\eta_{LAB} = 1$, respectively, and have been plotted at the centers of the bins. It becomes obvious that it will be quite difficult to distinguish between different gluon distributions in our proposed charm experiments. The situation would, however, become much better for a higher luminosity of, say, $\mathcal{L} = 1000/\text{pb}$ in which case the error bars would decrease by a factor 3.

We now briefly address the theoretical uncertainties of our results in Fig. 3 related to the dependence of the cross sections and asymmetries on the renormalization/factorization scale M . Since all our calculations could be performed in LO only, this is a particularly important issue. When using the scale $M = m_T$ it turns out that the cross sections in Fig. 3a are subject to changes of about 10% at $p_T < 15$ GeV, and of as much as 20 – 25% at larger p_T . Changes of in most cases below 10% are found for the η_{LAB} -curves in Fig. 3c. In contrast to this (not unexpected) fairly strong scale dependence of the polarized cross sections, the *asymmetries*, which will be the quantities actually measured, are very insensitive to scale changes, deviating usually by not more than a few percent from the values shown in Fig. 3b,d for all relevant p_T and η_{LAB} . This finding seems important in two respects: Firstly, it warrants the genuine sensitivity of the asymmetry to Δg , implying that despite the sizeable scale dependence of the cross section it still seems a reasonable and safe procedure to compare LO theoretical predictions for the asymmetry with future data and to extract Δg from such a comparison. Secondly, it sheds light on the possible role of NLO corrections to our results, suggesting that such corrections might be sizeable for the cross sections, but less important for the asymmetry.

4 Photoproduction of Jets

The generic cross section formula for the production of a single jet with transverse momentum p_T and rapidity η is similar to that in (5), the sum now running over all properly symmetrized $2 \rightarrow 2$ subprocesses for the direct ($\gamma b \rightarrow cd$) and resolved ($ab \rightarrow cd$) cases. When only light flavors are involved, the corresponding differential helicity-dependent LO subprocess cross sections can be found in [25]. In all following predictions we will deal with the charm contribution to the cross section by including charm only as a *final* state particle produced via the subprocesses $\gamma g \rightarrow c\bar{c}$ (for the direct part) and $gg \rightarrow c\bar{c}$, $q\bar{q} \rightarrow c\bar{c}$ (for the resolved part). For the values of p_T considered it turns out that the finite charm mass can be safely neglected. In all following applications we will use the renormalization/factorization scale $M = p_T$. We have again found that the scale dependence of the asymmetries is rather weak as compared to that of the cross sections.

It appears very promising [7] to study the η_{LAB} -distribution of the cross section and the asymmetry. The reason for this is that for negative η_{LAB} the main contributions are expected to come from the region $x_\gamma \rightarrow 1$ and thus mostly from the direct piece at $x_\gamma = 1$. To investigate this, Fig. 4 shows our results for the single-inclusive jet cross section and its asymmetry vs. η_{LAB} and integrated over $p_T > 8$ GeV for the four sets of the polarized proton's parton distributions. For Figs. 4a,b we have used the 'maximally' saturated set of polarized photonic parton densities, whereas Figs. 4c,d correspond to the 'minimally' saturated one. Comparison of Figs. 4a,c or 4b,d shows that indeed the direct contribution clearly dominates for $\eta_{LAB} \leq -0.5$, where also differences between the polarized gluon distributions of the proton show up clearly. Furthermore, the cross sections are generally large in this region with asymmetries of a few percents. At positive η_{LAB} , we find that the cross section is dominated by the resolved contribution

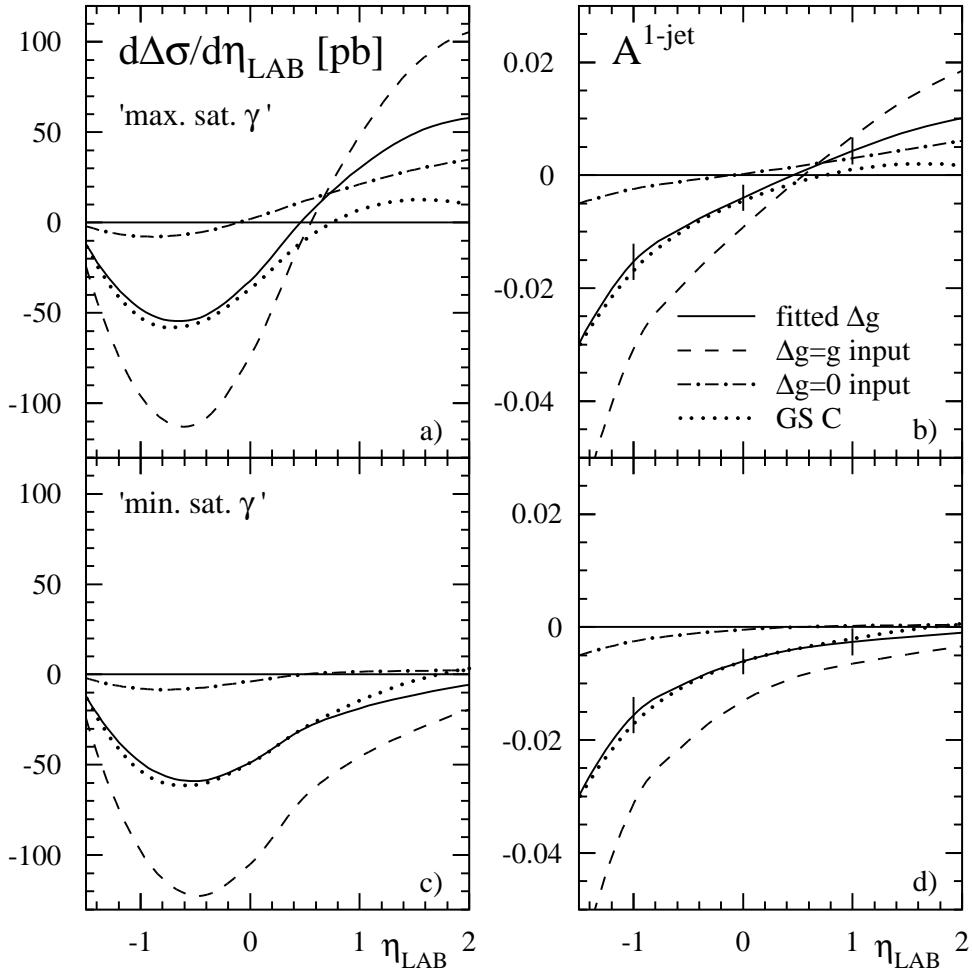


Figure 4: **a:** η_{LAB} -dependence of the polarized single-jet inclusive photoproduction cross section in ep -collisions at HERA, integrated over $p_T > 6$ GeV. The renormalization/factorization scale was chosen to be $M = p_T$. The resolved contribution to the cross section has been calculated with the 'maximally' saturated set of polarized photonic parton distributions. **b:** Asymmetry corresponding to **a**. The expected statistical errors have been calculated according to (6) and as described in the text. **c,d:** Same as **a,b**, but for the 'minimally' saturated set of polarized photonic parton distributions.

and is therefore sensitive to both the parton content of the polarized proton *and* the photon. This means that one can only learn something about the polarized photon structure functions if the polarized parton distributions of the proton are already known to some accuracy or if an experimental distinction between resolved and direct contributions can be achieved. We note that the dominant contributions to the resolved part at large η_{LAB} are driven by the polarized photonic *gluon* distribution Δg^γ . Again we include in Figs. 4b,d the expected statistical errors which we have estimated according to (6) with $P_e * P_p = 0.5$, $\mathcal{L} = 100/\text{pb}$, $\epsilon = 1$ for bins of $\Delta\eta_{LAB} = 1$. From the results it appears that a measurement of the proton's Δg should be possible from single-jet events at negative rapidities where the contamination from the resolved contribution is minimal.

In the unpolarized case, an experimental criterion for a distinction between direct and resolved contributions has been introduced [26] and used [4] in the case of dijet photoproduction

at HERA. We will now adopt this criterion for the polarized case to see whether it would enable a further access to Δg and/or the polarized photon structure functions. The generic expression for the polarized cross section for the photoproduction of two jets with laboratory system rapidities η_1, η_2 is to LO

$$\frac{d^3\Delta\sigma}{dp_T d\eta_1 d\eta_2} = 2p_T \sum_{f^e, f^p} x_e \Delta f^e(x_e, M^2) x_p \Delta f^p(x_p, M^2) \frac{d\Delta\hat{\sigma}}{d\hat{t}}, \quad (7)$$

where p_T is the transverse momentum of one of the two jets (which balance each other in LO) and

$$x_e \equiv \frac{p_T}{2E_e} (e^{-\eta_1} + e^{-\eta_2}) \quad , \quad x_p \equiv \frac{p_T}{2E_p} (e^{\eta_1} + e^{\eta_2}) \quad . \quad (8)$$

Following [4], we will integrate over the cross section to obtain $d\Delta\sigma/d\bar{\eta}$, where $\bar{\eta} \equiv (\eta_1 + \eta_2)/2$. Furthermore, we will apply the cuts [4] $|\Delta\eta| \equiv |\eta_1 - \eta_2| \leq 0.5$, $p_T > 6$ GeV. The important point is that measurement of the jet rapidities allows for fully reconstructing the kinematics of the underlying hard subprocess and thus for determining the variable [4]

$$x_\gamma^{OBS} = \frac{\sum_{jets} p_T^{jet} e^{-\eta^{jet}}}{2yE_e} \quad , \quad (9)$$

which in LO equals $x_\gamma = x_e/y$ with y as before being the fraction of the electron's energy taken by the photon. Thus it becomes possible to experimentally select events at large x_γ , $x_\gamma > 0.75$ [26, 4], hereby extracting the *direct* contribution to the cross section with just a rather small contamination from resolved processes. Conversely, the events with $x_\gamma \leq 0.75$ will represent the resolved part of the cross section. This procedure should therefore be ideal to extract Δg on the one hand, and examine the polarized photon structure functions on the other.

Fig. 5 shows the results [7] for the direct part of the cross section according to the above selection criteria. The contributions from the resolved subprocesses have been included, using the 'maximally' saturated set of polarized photonic parton densities. They turn out to be non-negligible but, as expected, subdominant. More importantly, due to the constraint $x_\gamma > 0.75$ they are determined by the polarized quark, in particular the u -quark, distributions in the photon, which at large x_γ are equal to their unpolarized counterparts as a result of the Q^2 -evolution (see Fig. 2), rather *independent* of the hadronic input chosen. Thus the uncertainty coming from the polarized photon structure is minimal here and under control. As becomes obvious from Fig. 5, the cross sections are fairly large over the whole range of $\bar{\eta}$ displayed and very sensitive to the shape *and* the size of Δg with, unfortunately, not too sizeable asymmetries as compared to the statistical errors for $\mathcal{L} = 100/\text{pb}$. A measurement of Δg thus appears to be possible under the imposed conditions only if luminosities clearly exceeding 100/pb can be reached. Fig. 6 displays the same results, but now for the resolved contribution with $x_\gamma \leq 0.75$ for the 'maximally' saturated set (Figs. 6a,b) and the 'minimally' saturated one (Figs. 6c,d). As expected, the results depend on both the parton content of the polarized photon and the proton, which implies that the latter has to be known to some accuracy to extract some information on the polarized photon structure. It turns out that again mostly the polarized *gluon* distribution of the photon would be probed in this case, in particular at $\bar{\eta} > 0.75$. Contributions from the Δq^γ are more affected by the x_γ -cut; still they amount to about 50% of the cross section at $\bar{\eta} = 0$. We finally emphasize that the experimental finding of a non-vanishing asymmetry here would establish at least the definite existence of a resolved contribution to the polarized cross section.

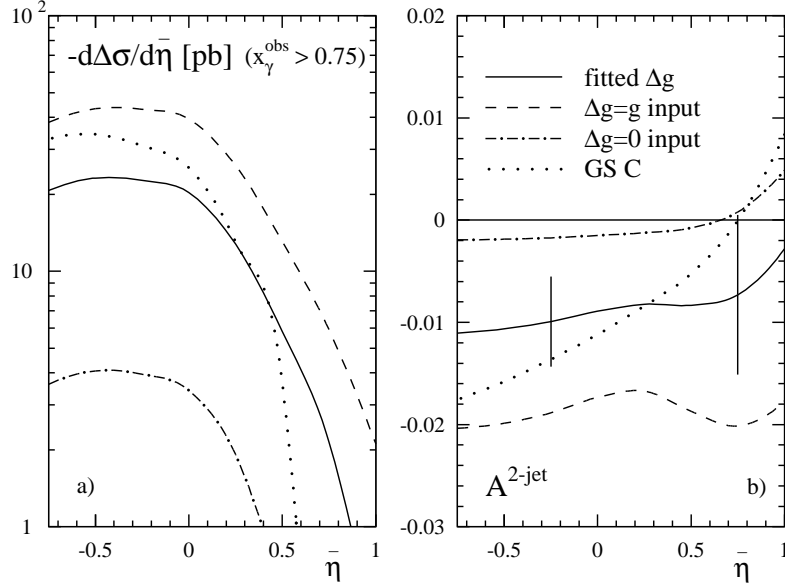


Figure 5: **a:** $\bar{\eta}$ -dependence of the 'direct' part of the polarized two-jet photoproduction cross section in ep -collisions at HERA for the four different sets of polarized parton distributions of the proton. The experimental criterion $x_\gamma^{OBS} > 0.75$ has been applied to define the 'direct' contribution (see text). The resolved contribution with $x_\gamma^{OBS} > 0.75$ has been included using the 'maximally' saturated set of polarized photonic parton distributions. **b:** Asymmetry corresponding to **a**. The expected statistical errors indicated by the bars have been calculated according to (6) and as explained in the text.

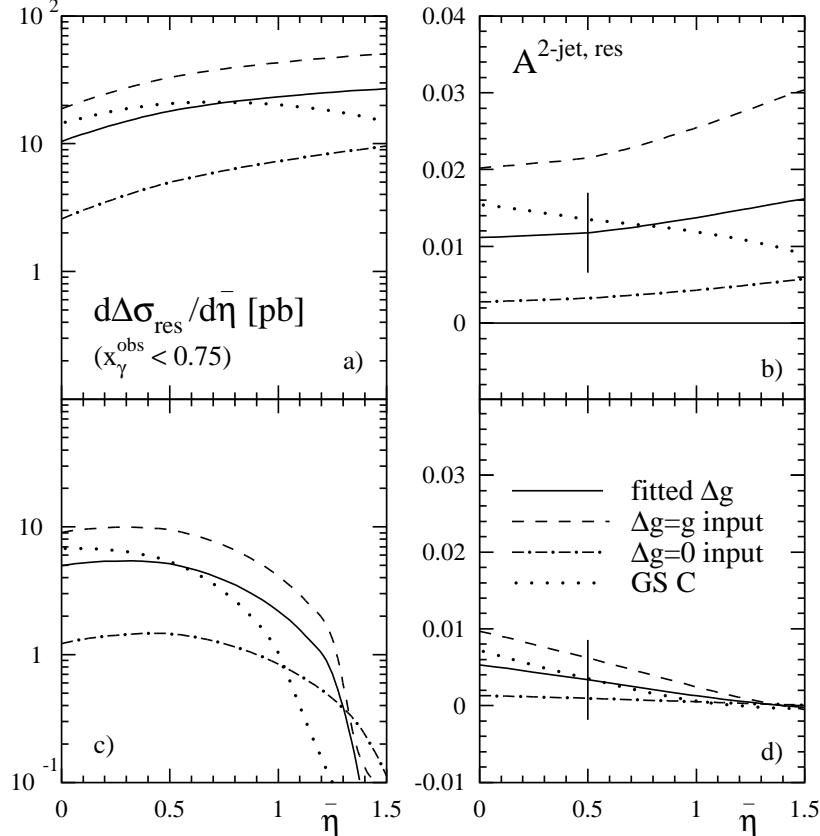


Figure 6: Same as Fig. 5, but for the resolved part of the cross section, defined by $x_\gamma^{OBS} \leq 0.75$ (see text). For **a,b**: the 'maximally' saturated set of polarized photonic parton distributions has been used and for **c,d** the 'minimally' saturated one.

5 Summary and Conclusions

We have analyzed various photoproduction experiments in the context of a polarized ep -collider mode of HERA. All of these have already been successfully performed in the unpolarized case at HERA. All processes we have considered have in common that they get contributions from incoming gluons already in the lowest order and thus look promising tools to measure the polarized gluon distribution of the proton. In addition, they derive their importance from their sensitivity not only to Δg , but also to the completely unknown parton content of the polarized photon entering via the resolved contributions to the polarized cross sections. As far as a 'clear' determination of Δg is concerned, this resolved piece, if non-negligible, might potentially act as an obstructing background, and it is therefore crucial to assess its possible size which we have done by employing two very different sets for the polarized photonic parton distributions. Conversely, and keeping in mind that HERA has been able to provide much new information on the unpolarized hadronic structure of the photon, it is also conceivable that photoproduction experiments at a polarized version of HERA could be *the* place to actually look for effects of the polarized photon structure and to prove the existence of resolved contributions to the polarized cross sections and asymmetries.

In the case of open-charm photoproduction we found that the resolved contribution is generally negligible except for the *total* charm cross section at HERA energies. Furthermore, the cross sections and their asymmetries are very sensitive to shape and size of Δg . We found, however, that very high luminosities, $\mathcal{L} = 1000/\text{pb}$, would be needed to measure the asymmetries with sufficient accuracy to decide between the various possible scenarios for Δg . Concerning photoproduction of jets, we find a generally much larger size of the resolved contribution. It turns out that the rapidity-distribution of the single-inclusive jet cross section separates out the direct part of the cross section at negative rapidities. In this region again a strong dependence on Δg is found with larger cross sections than for the case of charm production. The corresponding asymmetries clearly appear to be measurable here even for $\mathcal{L} = 100/\text{pb}$. At larger rapidities the cross section becomes sensitive to both the parton content of the polarized proton *and* photon, and an extraction of either of them does not seem straightforward. The situation improves when considering dijet production and adopting an analysis successfully performed in the unpolarized case [26, 4] which is based on reconstructing the kinematics of the underlying subprocess and thus effectively separating direct from resolved contributions. We find that in this case the (experimentally defined) direct contribution should provide access to Δg whereas the resolved part, if giving rise to a non-vanishing asymmetry, would establish existence of a polarized parton content of the photon. Again the corresponding measurements would require high luminosities since the involved asymmetries are rather small. The measurements we have proposed seem a very interesting challenge for a future polarized ep mode of HERA.

Acknowledgements

We are thankful to the members of the working group, in particular to J. Feltesse and M. Glück, for helpful discussions. The work of M.S. has been supported in part by the 'Bundesministerium für Bildung, Wissenschaft, Forschung und Technologie', Bonn.

References

- [1] I. Abt et al., H1 collab., Phys. Lett. **B314**, 436 (1993).
- [2] M. Derrick et al., ZEUS collab., Phys. Lett. **B342**, 417 (1995).
- [3] T. Ahmed et al., H1 collab., Nucl. Phys. **B445**, 195 (1995).
- [4] M. Derrick et al., ZEUS collab., Phys. Lett. **B348**, 665 (1995).
- [5] M. Derrick et al., ZEUS collab., Phys. Lett. **B349**, 225 (1995).
- [6] S. Aid et al., H1 collab., DESY 96-055.
- [7] M. Stratmann and W. Vogelsang, Univ. Dortmund report DO-TH 96/10 and Rutherford report RAL-TR-96-033, to appear in Z. Phys. **C**.
- [8] M. Glück, E. Reya, M. Stratmann and W. Vogelsang, Phys. Rev. **D53**, 4775 (1996).
- [9] T. Gehrmann and W.J. Stirling, Phys. Rev. **D53**, 6100 (1996).
- [10] A recent overview on the experimental status can be found, e.g., in R. Voss, in proceedings of the workshop on 'Deep Inelastic Scattering and QCD (DIS '95)', Paris, 1995, eds. J.F. Laporte and Y. Sirois.
- [11] R.D. Ball, S. Forte, and G. Ridolfi, Phys. Lett. **B378**, 255 (1996).
- [12] M. Glück, E. Reya, and A. Vogt, Z. Phys. **C67**, 433 (1995).
- [13] C.F. von Weizsäcker, Z. Phys. **88**, 612 (1934);
E.J. Williams, Phys. Rev. **45**, 729 (1934).
- [14] M. Klasen, G. Kramer and S.G. Salesch, Z. Phys. **C68**, 113 (1995);
M. Klasen and G. Kramer, Phys. Lett. **B366**, 385 (1996) and DESY 95-226.
- [15] M. Glück and W. Vogelsang, Z. Phys. **C55**, 353 (1992), Z. Phys. **C57**, 309 (1993).
- [16] M. Glück, M. Stratmann and W. Vogelsang, Phys. Lett. **B337**, 373 (1994).
- [17] M. Glück, E. Reya, and A. Vogt, Phys. Rev. **D46**, 1973 (1992).
- [18] see M. Arneodo et al., EMC, Z. Phys. **C35**, 1 (1987), and references therein.
- [19] M. Glück and E. Reya, Z. Phys. **C39**, 569 (1988).
- [20] M. Glück, E. Reya and W. Vogelsang, Nucl. Phys. **B351**, 579 (1991).
- [21] A.P. Contogouris, S. Papadopoulos and B. Kamal, Phys. Lett. **246**, 523 (1990);
M. Karliner and R.W. Robinett, Phys. Lett. **B324**, 209 (1994).
- [22] L.M. Jones and H.W. Wyld, Phys. Rev. **D17**, 759 (1978);
M. Glück, J.F. Owens and E. Reya, Phys. Rev. **D17**, 2324 (1978);
J. Babcock, D. Sivers and S. Wolfram, Phys. Rev. **D18**, 162 (1978);
B. Combridge, Nucl. Phys. **B151**, 429 (1979).
- [23] S. Frixione and G. Ridolfi, INFN-Genova report GEF-TH-4/1996, hep-ph 9605209.
- [24] G. Baum et al., COMPASS Collab., CERN/SPSLC 96-14.
- [25] J. Babcock, E. Monsay and D. Sivers, Phys. Rev. **D19**, 1483 (1979).
- [26] J.R. Forshaw and R.G. Roberts, Phys. Lett. **B319**, 539 (1993).